

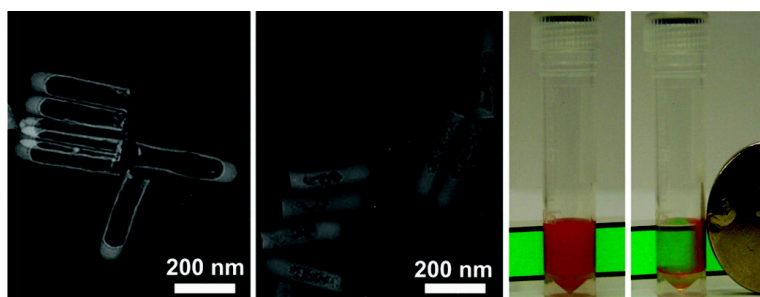
Communication

Magnetic Nanotubes for Magnetic-Field-Assisted Bioseparation, Biointeraction, and Drug Delivery

Sang Jun Son, Jonathan Reichel, Bo He, Mattan Schuchman, and Sang Bok Lee

J. Am. Chem. Soc., **2005**, 127 (20), 7316-7317 • DOI: 10.1021/ja0517365 • Publication Date (Web): 29 April 2005

Downloaded from <http://pubs.acs.org> on March 25, 2009



More About This Article

Additional resources and features associated with this article are available within the HTML version:

- Supporting Information
- Links to the 45 articles that cite this article, as of the time of this article download
- Access to high resolution figures
- Links to articles and content related to this article
- Copyright permission to reproduce figures and/or text from this article

[View the Full Text HTML](#)



Magnetic Nanotubes for Magnetic-Field-Assisted Bioseparation, Biointeraction, and Drug Delivery

Sang Jun Son, Jonathan Reichel, Bo He, Mattan Schuchman, and Sang Bok Lee*

Department of Chemistry & Biochemistry, University of Maryland, College Park, Maryland 20742

Received March 18, 2005; E-mail: slee@umd.edu

Magnetic particles have been extensively studied in the field of biomedical and biotechnological applications, including drug delivery, biosensors, chemical and biochemical separation and concentration of trace amounts of specific targets, such as bacteria or leukocytes, enzyme encapsulation, and contrast enhancement in magnetic resonance imaging (MRI).^{1–3} In most applications, spherical nanoparticles have been used. However, spherical magnetic nanoparticles still need to be improved for controlling particle sizes, surface functionalizations, and their environmental compatibility due to the structural limitation of spherical particles when multifunctionality is required on their surfaces.

Since Martin and co-workers have demonstrated the differential functionalization of silica nanotubes,⁴ tubular structure of nanoparticles has become highly attractive for the multifunctional nanoparticles due to their structural attributes, such as the distinctive inner and outer surfaces, over conventional spherical nanoparticles. Inner voids can be used for capturing, concentrating, and releasing species ranging in size from large proteins to small molecules because tube dimensions can be easily controlled by the template synthesis. Distinctive outer surfaces can be differentially functionalized with environment-friendly and/or probe molecules to a specific target. Therefore, by combining the attractive tubular structure with magnetic property, the magnetic nanotube (MNT) can be an ideal candidate for the multifunctional nanomaterial toward biomedical applications, such as targeting drug delivery with MRI capability. In this communication, we describe the synthesis of MNTs and their uses for magnetic-field-assisted chemical and biochemical separations, immunobinding, and drug delivery.

We synthesized silica nanotubes with a layer of magnetite (Fe₃O₄) nanoparticles on the inner surface of the nanotube using porous alumina film as template (60 and 200 nm pore diameters). Silica nanotubes were prepared in the pores of the template film by the previously reported “surface sol–gel” methods.^{5,6} To form the layer of magnetite nanoparticles, the silica nanotube alumina film was dip-coated with a 4:1 mixture solution of 1 M FeCl₃ and 2 M FeCl₂, dried in an Ar stream, immersed in 1 M NH₄OH for 5 min, and washed thoroughly with deionized water.⁷ For the differential functionalization of MNTs, the inner nanotube surface was treated with octadecyltriethoxysilane (C18-silane) while MNTs were still embedded in the pores of the alumina template. Free-standing MNTs were obtained after polishing both sides of the template film mechanically and dissolving the alumina template in a 0.1 N NaOH solution. After the template was dissolved completely, MNTs were collected by filtration.

Transmission electron microscopy (TEM) images of MNTs (Figure 1B,D) show clearly the magnetite layers on the inner surface of the nanotubes, while bare silica nanotubes have smooth tubular wall surfaces (Figure 1A,C). Figure 1E shows the room-temperature magnetization curves of MNTs obtained by a superconducting quantum interference device (SQUID). Both 60 and 200 nm diameter MNTs exhibit the superparamagnetic characteristics. Their

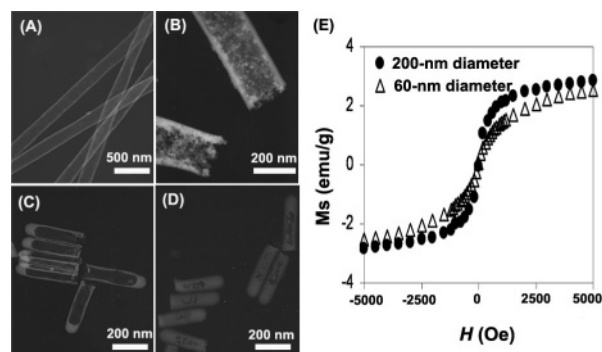


Figure 1. Transmission electron micrographs (TEM) of 200 nm (A, B) and 60 nm (C, D) diameter silica nanotubes without magnetite (A, C), and magnetic nanotubes (MNTs) with magnetite (B, D); (E) room-temperature magnetization curves of MNTs.

saturation magnetizations are 2.7 and 2.9 emu/g, respectively. These values are in accordance with previously reported data for silica–magnetite nanoparticles.⁸ For further analysis, energy-dispersive X-ray (EDX) and field emission scanning electron microscopy (FESEM) analyses were carried out (see Supporting Information for details).

For an exemplary chemical extraction and separation experiment, MNTs ($\sim 10^9$) with C18-functionalized inside were added to a solution of 1,1'-dioctadecyl-3,3,3',3'-tetramethylindocarbocyanine perchlorate (DiIC₁₈, 38 μ M) in water/methanol (9:1 v/v, 1 mL). The mixture was shaken and 10 min allowed for these dye molecules to enter the MNTs by the strong hydrophobic interaction. These nanotubes are completely suspendible in aqueous phases (even in pure water) due to their outer hydrophilic silica surfaces. A Nd–Fe–B magnet (ca. 0.3 T) was then used to separate the nanotubes and, thus, the DiIC₁₈ molecules from the solution. Figure 2A,B shows that magnetic separation makes a solution, which initially contains red color dye (DiIC₁₈), almost transparent and clear. UV–vis spectroscopy and fluorescence microscopy studies were further performed to show that more than 95% of the DiIC₁₈ was removed from the solution and that the hydrophobic dye was extracted into the MNTs (see Supporting Information for details). As a control experiment, when MNTs without a C-18 layer inside were incubated with DiIC₁₈, no detectable change was observed. The above results tell us that these MNTs can be used for the extraction, separation, release, and analysis of trace amounts of the extremely hydrophobic toxic chemicals, such as polychlorinated biphenyls (PCBs) and polycyclic aromatic hydrocarbons (PAHs) in water.⁹

MNTs with human IgG inside were prepared and added to the mixed solution (2 mL, pink color) of fluorescein-labeled anti-bovine IgG (green, 0.71 μ M in 0.1 M phosphate-buffered saline (PBS), pH 7.4) and Cy3-labeled anti-human IgG (red, 0.67 μ M) in order to show a magnetic bioseparation using antigen–antibody interac-

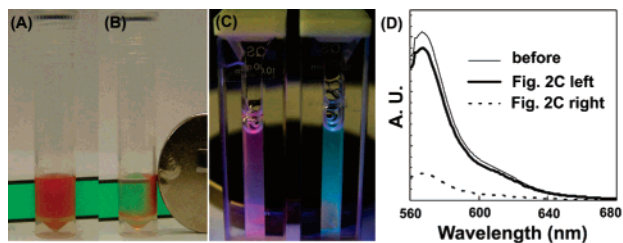


Figure 2. Pictures of vial containing 38 μM DiIC18 and 10^9 C-18-modified MNTs before (A) and after (B) magnetic separation for 2 min; (C) a picture of the solution containing green FITC-labeled anti-bovine IgG and red Cy3-labeled anti-human IgG after magnetic separation. Each solution was incubated with BSA-MNTs (left) and MNTs with human IgG inside (right) before magnetic separation. (D) Fluorescence spectra ($\lambda_{\text{ex}} = 552$ nm) corresponding to Figure 2C for measuring the amount of remaining red Cy3-labeled anti-human IgG in solution.

tion.⁴ BSA-derivatized MNTs (BSA-MNTs) were prepared as well to show a nonspecific biointeraction. The outer surfaces of all the MNTs were functionalized with poly(ethylene glycol) (PEG) silane to protect nonspecific adsorptions on silica surfaces. Figure 2C shows, after magnetic separation, the solution changes from the original pink to greenish–blue only when MNTs with human IgG inside are added, while the solution with BSA-MNTs remains its original pink color. This means that red Cy3-labeled anti-human IgG was separated specifically from the solution by human IgG-MNTs. Fluorescence spectra (Figure 2D) show that 84% of Cy3-labeled anti-human IgG was separated by human IgG-MNTs but only 9% by BSA-MNTs.

Very interestingly, the magnetic property of MNTs can be used to facilitate and enhance biointeractions between the outer surfaces of MNTs and a specific target surface. As a potential application, the drug delivery efficiency might be greatly improved by the magnetic-field-assisted biointeraction when the MNTs carry the drug inside and have probe molecules, such as antibody, on the outer surfaces. For a proof-of-concept experiment, onto the anti-rabbit IgG-modified glass slide were added 60 nm diameter MNTs with an FITC-modified inner surface and a rabbit IgG-modified outer surface, and they were incubated for 10 min with and without magnetic field from the bottom of the glass slide. After washing the unbound nanotubes, the number of bound nanotubes was counted at five different regions of fluorescence microscopy images (Figure 3A,B) and averaged. About 4.2-fold binding enhancement was observed for the antigen–antibody interactions in the presence of magnetic field, and this means that we can control the efficiency of antigen–antibody interactions spatially by means of an external magnetic field.

5-Fluorouracil (5-FU), 4-nitrophenol, and ibuprofen were loaded as model drug molecules into the pores of MNTs functionalized with amino–silane (aminopropyl triethoxysilane, APTS) to study the effect of the charged hydrogen-bonding interaction between drug and the inner pore surfaces on loading and release.¹⁰ The amine-functionalized MNTs were immersed in the hexane (ibuprofen) or ethanol (5-FU, 4-nitrophenol) solutions of drugs. The amine functional groups make strong ionic and/or hydrogen-bonding interactions with the acid functional groups of drug molecules. UV–vis spectrophotometer study showed that $\sim 10^7$ ibuprofen molecules per nanotube were loaded, as well as $\sim 10^6$ 4-nitrophenol and $\sim 10^7$ 5-FU. The value for ibuprofen is about twice the monolayer

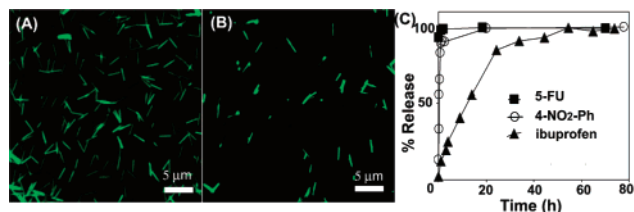


Figure 3. Fluorescence microscope image of bound MNTs (60 nm diameter, 3 μm length), which have an FITC-modified inner surface and a rabbit IgG-modified outer surface, to the surface of anti-rabbit IgG-modified glass after antigen–antibody interaction with (A) and without (B) magnetic field under the glass substrate. All of the long bright spots in A and B are the individual nanotubes. Some brighter nanotubes in the images may be caused by the aggregation of two or three nanotubes. (C) In vitro release of ibuprofen, 4-nitrophenol (4-NO₂Ph), and 5-fluorouracil (5-FU) from MNTs (60 nm diameter, 250 nm length).

coverage of the MNT inner surface. The release tests were performed in 1 mL of pH 7.4 PBS (Figure 3C). It was observed that less than 10% of ibuprofen was released in 1 h, and 80% was released after 24 h. In the cases of 5-FU and 4-nitrophenol, however, more than 90% was released in 1 h. These results tell us that the carboxylic acid group of ibuprofen makes the strongest interaction with the amine group inside MNT and ibuprofen released with a slow rate.

We want to again emphasize that the hollow tubular structure of a magnetic particle can be one of the most promising candidates for various applications, including chemical and biochemical separations and drug delivery. We believe that MNTs with drug-friendly interiors and target-specific exteriors can open a new field in material for the multifunctional targeted drug delivery.¹¹

Acknowledgment. This work was supported by the Laboratory for Physical Sciences and University of Maryland. We thank Dr. R. Greene and Dr. B. Liang for valuable assistance with SQUID, and Tim Mangel for EDX measurement.

Supporting Information Available: EDX and FESEM of MNTs, UV–vis spectrum for DiIC₁₈ separation, and procedure for antibody immobilization (PDF). This material is available free of charge via the Internet at <http://pubs.acs.org>.

References

- (1) Martin, C. R.; Kohli, P. *Nat. Rev. Drug Discovery* **2003**, *2*, 29.
- (2) Huang, Y.; Nan, A.; Rosen, G. M.; Winanski, C. S.; Schneider, E.; Isai, P.; Ghandehari, H. *Macromol. Biosci.* **2003**, *3*, 647.
- (3) Bucak, S.; Jones, D. A.; Laibinis, P. E.; Hatton, T. A. *Biotechnol. Prog.* **2003**, *19*, 477.
- (4) (a) Mitchell, D. T.; Lee, S. B.; Trofin, L.; Li, N.; Nevanen, T. K.; Soderlund, H.; Martin, C. R. *J. Am. Chem. Soc.* **2002**, *124*, 11864. (b) Okamoto, K.; Shook, C. J.; Bivona, L.; Lee, S. B.; English, D. S. *Nano Lett.* **2004**, *4*, 233.
- (5) (a) Kovtyukhova, N. I.; Mallouk, T. E.; Mayer, T. S. *Adv. Mater.* **2003**, *15*, 780. (b) Steinle, E. D.; Mitchell, D. T.; Wirtz, M.; Lee, S. B.; Young, V. Y.; Martin, C. R. *Anal. Chem.* **2002**, *74*, 2416.
- (6) Hornyak, G. L.; Patrissi, C. J.; Martin, C. R. *J. Phys. Chem. B* **1997**, *101*, 1548.
- (7) Breitzer, J.; Lisensky, G. *J. Chem. Educ.* **1999**, *76*, 943.
- (8) Yang, H.; Zhang, S.; Chen, X.; Zhung, Z.; Xu, J.; Wang, X. *Anal. Chem.* **2004**, *76*, 1316.
- (9) Buehler, S. S.; Basu, I.; Hites, R. A. *Environ. Sci. Technol.* **2001**, *35*, 2417.
- (10) (a) Lee, S. B.; Hong, J.-I. *Tetrahedron Lett.* **1996**, *37*, 8501. (b) Vallet-Regi, M.; Ramila, A.; Real, P.; Perez-Pariente, J. *Chem. Mater.* **2001**, *13*, 308.
- (11) Ferrari, M. *Nat. Rev.* **2005**, *5*, 1.

JA0517365